Evidence and evaluation of the Bychkov-Rashba effect in SiGe/Si/SiGe quantum wells

Z. Wilamowski,[1,2] W. Jantsch,[1] H. Malissa,[1] and U. Rössler[3]
[1]*Institut für Halbleiterphysik, Johannes Kepler Universität, A-4040 Linz, Austria*
[2]*Institute of Physics, Polish Academy of Sciences, Al Lotnikow 32/46, PL 0668 Warsaw, Poland*
[3]*Institut für Theoretische Physik, Universität Regensburg, D-93040 Regensburg, Germany*
(Received 17 December 2001; revised 19 August 2002; published 15 November 2002)

From spin resonance of two-dimensional (2D) conduction electrons in a modulation doped SiGe/Si/SiGe quantum well structure we find a 2D anisotropy of both the line broadening (dephasing time) and the *g* factor. Both can be explained consistently employing the Bychkov-Rashba (BR) term $\mathscr{H}_{\mathrm{BR}}=\alpha(\mathbf{k}\times\sigma)\cdot\mathbf{e}_z$, which turns out here to be the dominant coupling between electron orbital motion and spin. We obtain a BR parameter of $\alpha=0.55\times10^{-12}$ eV cm—three orders of magnitude smaller than in quantum well structures based on III-V semiconductors, consistent with the much smaller spin-orbit coupling in Si.

DOI: 10.1103/PhysRevB.66.195315 PACS number(s): 72.25.Rb, 73.21.Fg, 85.75.−d

I. INTRODUCTION

Present attempts to realize an electronic device based on the spin of electrons instead of its charge has stimulated intensive investigations of spin properties in relation to the electronic properties. Conduction electrons are natural candidates for such devices, especially in low-dimensional systems, where electrons can easily be manipulated by applied voltages or by illumination with light. For two-dimensional electron systems (2DES) it has already been shown that the electrical conductivity depends on the spin polarization.[1,2,3] Thus, in principle, electrical measurements are capable to detect the spin state of a 2DES. In this context the Bychkov-Rashba (BR) term[4,5] $\mathscr{H}_{\mathrm{BR}}=\alpha(\mathbf{k}\times\sigma)\cdot\mathbf{e}_z$ has recently received much attention. Here $\mathbf{k}$ is the in-plane momentum of the 2D electron, σ the vector of the Pauli spin matrices, $\mathbf{e}_z$ the symmetry axis of the quantum well structure, and α is a parameter that depends on the geometry of the quantum well, potential gradients and on the composition of well and barriers. The BR term couples spin and orbital motion of the confined carriers. It has been proposed as a method to manipulate spins as required for spin transistors[6] or quantum computing[7] in materials with large α. On the other hand, since the BR term leads to an additional channel for spin lattice relaxation,[8] materials with small α are preferable if long spin lifetimes are needed. The role of the BR term has been extensively studied also in the context of the metal-to-insulator transition in the 2DES.[9,10]

In this paper we employ high-resolution conduction electron spin-resonance (CESR) to study the effect of the carrier concentration n_s on the spin properties of 2D electrons in Si quantum wells embedded in SiGe barriers. We find an anisotropy both in the *g* factor and in the CESR linewidth that increases with increasing n_s. This effect is explained by invoking the BR term. The material- and geometry-specific weighting factor α is extracted here from the measured anisotropies. As it turns out from our investigation, CESR is a very sensitive tool to evaluate the BR spin-orbit coupling quantitatively. Its sensitivity is by orders of magnitude higher than that of methods based on (i) beating effects in magneto oscillations,[11,12] (ii) Raman scattering,[13] or (iii) the investigation of weak localization,[14,15] which were applied to quantum structures based on III-V semiconductor where the zero field spin splitting is much bigger. To our knowledge the present study is the first one that invokes the BR term to interpret spin-orbit effects in modulation doped quantum well structures based on materials (such as Si and Ge) having a center of inversion.

II. EXPERIMENT

We investigate modulation doped Si quantum well samples grown by MBE on 1000 Ω cm, (100) Si substrates. The layer sequence and the conduction band edge are indicated schematically in Fig. 1. First, a graded buffer layer of $Si_{1-x}Ge_x$ is deposited that, owing to its thickness of 2.5 μm, is relaxed. On top of this, a pseudomorphic layer of Si ($d=12-20$ nm) is grown which finally forms the quantum well. This quantum well is strained due to the larger lattice constant of the relaxed buffer material, which splits the six equivalent Δ_1 conduction band minima into two with their main axis of the constant energy ellipsoids along growth direction and four ellipsoids with their main axes in-plane. Since the valleys oriented perpendicular to the interface are lower in energy, only these are populated. Therefore conduction electrons in the channel exhibit only the transverse mass ($m^*=0.19\,m_0$) and thus high mobility. The latter is limited at low temperatures by the ionized donors which are accom-

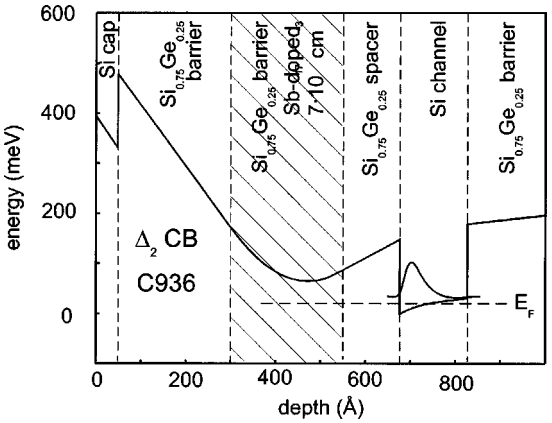

FIG. 1. Sample structure, for details see text. The conduction band edge and the electron density in the ground state of the 2DES are indicated.

modated in a doping layer, separated from the quantum well by the second barrier formed by $Si_{1-x}Ge_x$ ($x=0.25$) of 12 nm thickness. The doping layer has the same composition, but contains typically 7×10^{17} cm^{-3} of Sb. Finally another undoped $Si_{1-x}Ge_x$ layer and a cap layer is deposited. The same type of samples was used in Ref. 3 where also the mobility of the 2D carriers was discussed: at low temperatures mobilities of up to 200 000 cm^2/V s at 2 K were observed at electron densities exceeding 3×10^{11} cm^{-2}.

In this paper, three samples with different donor concentrations were investigated. The one with the higher concentration exhibited a constant n_s of 4×10^{11} cm^{-2}. Two others, with lower donor concentration, showed complete carrier freeze-out below 40 K and strong persistent photoconductivity upon illumination with band gap light. This enabled us to increase the electron concentration in the quantum well stepwise by short illumination up to a saturation value of 7×10^{11} cm^{-2}. The change in electron concentration is accompanied by a change of electron mobility. Thus we are able to investigate the dependence of spin relaxation on the Fermi k vector and on the momentum scattering rate.

We investigate ESR in a standard Bruker X-band instrument operating at a frequency close to 9.44 GHz. We use a rectangular TE201 cavity where the sample is placed as close as possible to the nodal plane of the electric microwave field where the magnetic field is maximum. As usual, the static magnetic field is modulated, in our case with a frequency of 6 kHz and an amplitude of down to 1 μT allowing us to resolve the narrow lines due to the CESR. In the detection system a lock-in amplifier is used. The signal obtained is proportional to the derivative of the microwave absorption with respect to the magnetic field. Typical spectra are given in Fig. 2 for different orientations of the external static magnetic field. In this standard ESR experiment we observe the CESR of the high mobility 2DES (inset to Fig. 2) and simultaneously its cyclotron resonance (CR).[3,16] The latter allows us to determine the carrier density n_s and the momentum relaxation rate τ_k *in situ*.[16] Making use of the persistent photoconductivity in our structures[16] we follow the dependence of CESR parameters on k_F, and also on the direction of applied magnetic field, momentum relaxation rate $1/\tau_k$ and sample temperature.

In Fig. 3 the CESR linewidth is plotted for two different orientations of the magnetic field as a function of temperature. Practically no influence of temperature is observed on the linewidth if the magnetic field is oriented parallel to the layer plane ($\Theta=90°$). For perpendicular orientation [field applied parallel to the growth direction ($\Theta=0°$)], the observed line is very narrow and additional narrowing is observed with increasing temperature. The resonance field is practically temperature independent in the whole range of temperatures investigated—from 2 to 50 K. As can be seen in Fig. 2, both the resonance field and the linewidth depend on the direction of applied field. The magnitude of these anisotropies change from sample to sample and depend on the electron concentration.

Experimental results for the electron g factor are given in Fig. 4. The g factor for a magnetic field perpendicular to the layer ($\Theta=0$) is bigger than for in-plane orientation. The g factor is practically temperature independent in the whole range of temperatures investigated—from 2 to 50 K. The anisotropy of the g factor $\Delta g=g(0°)-g(90°)$, is shown in Fig. 4(a) as a function of n_s and in Fig. 4(b) its mean value, defined as $\langle g\rangle=[g(0°)+2g(90°)]/3$ is plotted. Both quantities vary linearly with n_s. Qualitatively the same behavior was reported in Ref. 2.

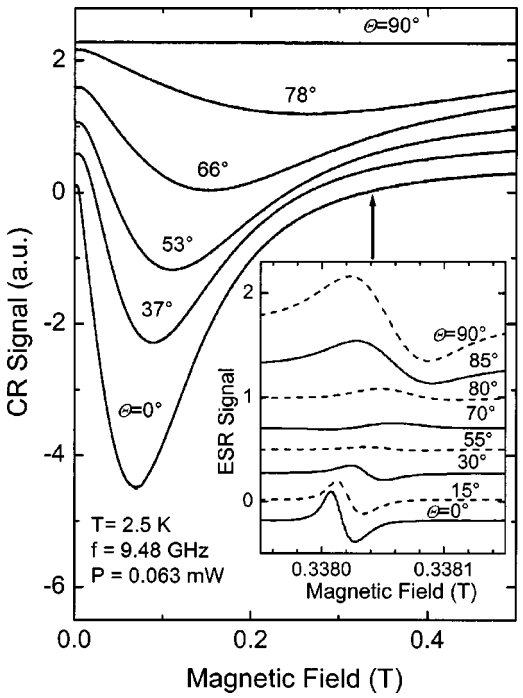

FIG. 2. Cyclotron resonance signal (first derivative with respect to magnetic field) for different angles of the applied static magnetic field as observed in a conventional ESR spectrometer. The inset shows with strong magnification the region around $g=2$ that corresponds to the conduction electron spin resonance. Temperature, microwave frequency, and power are indicated.

The CESR of 2D electrons in Si/SiGe structures is char-

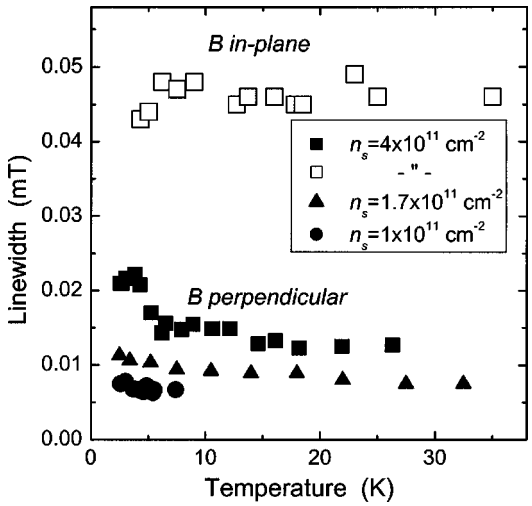

FIG. 3. CESR linewidth as a function of temperature for different electron densities and in-plane and perpendicular orientations of the magnetic field.

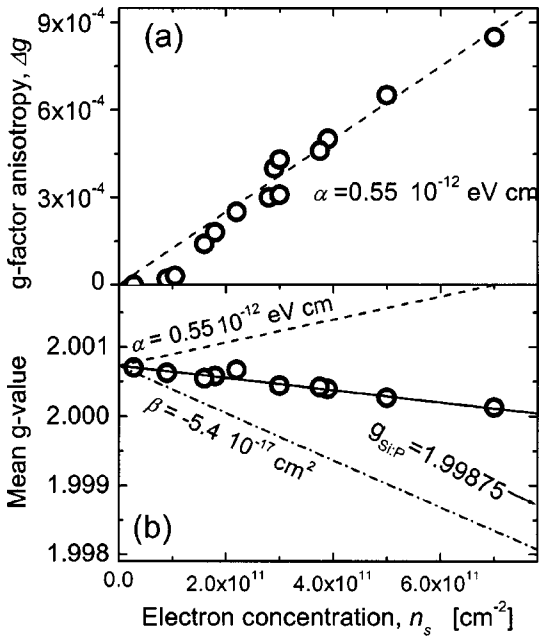

FIG. 4. (a) Measured g-factor anisotropy (circles), $\Delta g = g(0°) - g(90°)$ vs electron concentration. Dashed line: fit resulting in a BR parameter of $\alpha = 0.55 \times 10^{-12}$ eV cm. (b) Mean g value. Dashed line: Rashba contribution obtained with the same α parameter as in (a), dash-dotted line: effect of nonparabolicity with β adjusted to achieve agreement of the combination of the two effects with experiment (full line).

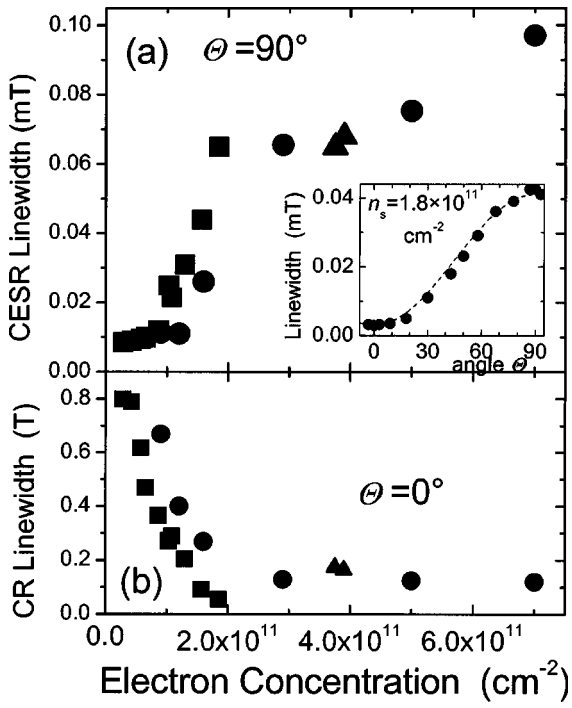

FIG. 5. (a) CESR linewidth for in-plane magnetic field. The inset shows the angular dependence of the linewidth. (b) Cyclotron resonance linewidth for perpendicular magnetic field.

acterized by a very narrow linewidth ΔH, which depends on the direction of applied magnetic field. For in-plane orientation the line width is typically of the order of 50 μT, but for perpendicular orientation the linewidth becomes smaller by an order of magnitude. The narrowest linewidth we observed is 3.4 μT (see Figs. 2 and 3), about two orders of magnitude narrower[16,17] than that of typical ESR lines of defects in Si. The line width at 1.9 K for in-plane orientation is plotted in Fig. 5(a) as a function of n_s. We find (see below) that this line width, expressed usually by the transverse relaxation rate Δ_2 (which is the inverse dephasing time) for $\Theta < 90°$ exceeds the one caused by finite spin lifetime $\Delta_1 = 1/\tau_s < \Delta_2$. For metals, the opposite is true since the spin lifetime (the longitudinal spin relaxation) is limited rather by momentum scattering. In our samples this is apparently not the case because of the high mobility. Only for Θ close to 0° the line width is limited by Δ_1 (see below).

In order to test the mechanism of spin relaxation we investigate also the momentum scattering rate which manifests itself in the CR linewidth. Figure 5(b) shows the CR linewidth as a function of n_s as obtained from three samples with different doping concentrations.[3,16] For low n_s, close to the metal-to-insulator transition, the CR linewidth shows a tendency to diverge as the potential fluctuations diverge due to breakdown of screening.[3]

III. MODEL AND DISCUSSION

Usually, the discussion of the resonance field and of the linewidth requires a complex analysis of various mechanisms. In the case of Si, however, the concentration of isotopes with nonzero nuclear spin is very small and the spin orbit coupling of conduction electrons is very weak. As a consequence, the g factor is very close to 2 and the common mechanisms of line broadening, caused by spin-phonon and hyperfine coupling, are negligible. As we show below, all our observations can be well described considering weak spin-orbit (SO) interaction. The isotropic part of SO coupling shifts the g factor. The pronounced g factor and linewidth anisotropies, however, can be described by the Bychkov-Rashba term that exists here because of the structure induced loss of mirror symmetry due to one-sided modulation doping of our samples.

A. The Bychkov-Rashba field

The most general form of spin-orbit coupling can be formulated as $(\nabla V \times \mathbf{p}) \cdot \sigma$, which is a scalar product of two pseudovectors (the vector product of a potential gradient with the particle momentum $\mathbf{p}$ and the vector of Pauli spin matrices σ). For a QW structure, ∇V can be identified with the built-in electric field (parallel to $\mathbf{e}_z$) and $\mathbf{p} = \mathbf{k}$ with the in-plane momentum of the confined particle. Thus we arrive at the form $\mathcal{H}_{BR} = \alpha(\mathbf{k} \times \sigma) \cdot \mathbf{e}_z$ as originally postulated by Bychkov and Rashba.[4,5] $\mathcal{H}_{BR}$ causes a spin-splitting of electronic states already in the absence of an external magnetic field. Spin degeneracy is a consequence of simultaneous spatial and time inversion symmetry as, e.g., in bulk Si or Ge. Here the spatial inversion symmetry is broken, however, by the formation of a noncentrosymmetric SiGe/Si/SiGe QW structure with single-sided doping. The overall symmetry of such a QW's is C_{4v},[18] which is also the group of the wave

vector at the conduction band minimum in bulk Si. The Hamiltonian in all its terms has to be invariant under this symmetry group, as it is the case for $(\mathbf{k}\times\sigma)\cdot\mathbf{e}_z = k_x\sigma_y - k_y\sigma_x$. Therefore such a term may exist in sample structures such as ours. The Zeeman splitting in an external magnetic field $\mathbf{H}_{ex}$ is in competition with the BR splitting: for large $\mathbf{H}_{ex}$, the former dominates while the latter survives[19] for $\mathbf{H}_{ex}\rightarrow 0$.

The 2DES constitutes a Pauli paramagnet and thus CESR detects only electrons close to the Fermi energy. The latter increases with increasing carrier concentration n_s. The Fermi surface of a 2DES is a circle with radius $k_F = \sqrt{2\pi n_s}$. The Fermi vector k_F enters the Rashba term in $\mathscr{H}_{BR}$ and increases with n_s. Thus the dependence of essential spin properties such as the g factor and the CESR linewidth on n_s should bear information on the BR spin-orbit coupling. We quantify this by dividing $\mathscr{H}_{BR}$ by $g_0\mu_B$ to convert it into a magnetic field $\mathbf{H}_{BR}=(2\alpha k_F/g_0\mu_B)\mathbf{e}_k\times\mathbf{e}_z$ that can be compared with the external field $\mathbf{H}_{ex}$ which rules the Zeeman splitting. Here, g_0 is the g factor and μ_B the Bohr magneton.

By definition, the BR field acts on the spin splitting but it does not affect the orbital motion. Because of that the BR and the external fields can be treated as additive only in the case when the cyclotron motion and thus the diamagnetic quantization can be neglected. As it is shown below, in that case a simple analysis of the effect of the BR term of the CESR is possible. In our samples, Shubnikov de Haas oscillations occur only at magnetic fields of more than 1.5 T which exceed that of CESR a few times even for the highest mobilities that occur for high carrier density. The apparent discrepancy of a high threshold field and high mobility can be resolved in terms of dominant small angle scattering that results from smooth potential fluctuations due to remote ionized donors.[3] This small angle scattering disturbs the CR but has little influence on the mobility. In this situation the approximation of weakly scattered plane waves with well defined k vectors appears more appropriate as compared to the rigorous analysis in the presence of well defined Landau states which is necessary for strongly quantizing magnetic field.[20] Therefore in the present case, the external field and the Rashba field can be added to describe their effect on a particular electron. For in-plane orientation of the applied field, Landau quantization for the 2DES vanishes and thus the approach of the additive BR field becomes exact.

B. Effective g factor

The effective g factor given in Fig. 4 was evaluated as usual from the externally applied field $\mathbf{H}_{ex}$ at which resonance occurs and from the microwave frequency. In the presence of the BR field $\mathbf{H}_{BR}$, however, the resonance condition takes the form $\hbar\omega = g_0\mu_B|\mathbf{H}_{eff}|$, where g_0 is the ''true,'' internal electron g factor that is obtained if the effective magnetic field $\mathbf{H}_{eff}=\mathbf{H}_{ex}+\mathbf{H}_{BR}$ is considered. When the external field $\mathbf{H}_{ex}$ is applied at an angle Θ and $\mathbf{H}_{BR}$ is distributed in the surface of the layer, then the value of $\mathbf{H}_{eff}$ is distributed around its mean value $\langle\mathbf{H}_{eff}\rangle$. For $\mathbf{H}_{BR}\ll\mathbf{H}_{ex}$, the variance of the distribution of the effective local field, which contributes to the linewidth broadening, is

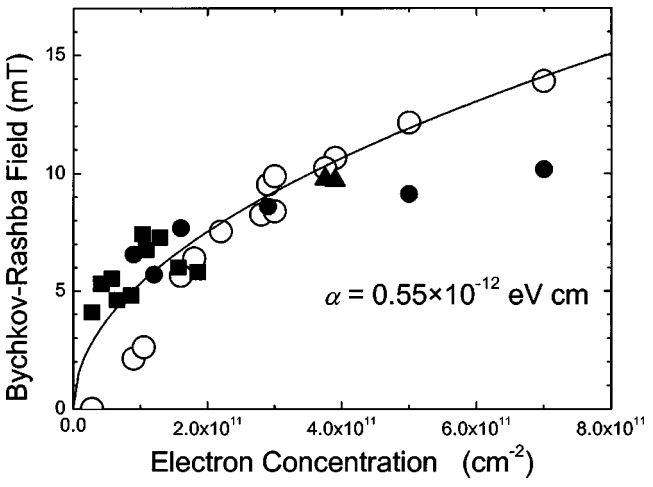

FIG. 6. BR field, as evaluated from the linewidth (■) and from the g-factor anisotropy (○) as a function of the density of a 2DES. The solid line is calculated with α as fitting parameter.

$$\delta H_{BR}^2 = \frac{1}{2} H_{BR}^2 \sin^2\Theta. \tag{1}$$

In order to model the g-factor we have to consider the degeneracy of the 2DES. The observable g factor corresponds to the g value at k_F only. Averaging for all possible directions of $\mathbf{k}_F$, the dependence of the measured g factor on the electron concentration n_s and on the direction of the external magnetic field is obtained as

$$g(n_s,\Theta) = g_0\frac{\langle H_{eff}\rangle}{H_{ex}} \cong g_0\left(1+\frac{H_{BR}^2}{4H_{ex}^2}(1+\cos^2\Theta)\right). \tag{2}$$

Equation (2) shows that the BR coupling leads to a g-factor anisotropy that is proportional to n_s. From the observed g-factor anisotropy [Fig. 4(a)] we are thus able to extract H_{BR} without any adjustable parameters and the results are given in Fig. 6 as a function of n_s (open symbols). The solid line in Fig. 6 is obtained using $\alpha = 0.55\times10^{-12}$ eV cm as a fitting parameter. Some variation of the BR coefficient α. could be expected with n_s as the potential gradient in the quantum well is changed. As it turns out, these deviations are below the sensitivity of our experiment, however, as can be seen in Figs. 4(a) and 6. For $n_s = 4\times10^{11}$ cm^{-2}, the value of α obtained gives a Rashba field of $H_R = 100$ G which yields a zero-field splitting of a few μeV, about three to four orders of magnitude smaller than for InAs wells.[11]

The dashed line in Fig. 4(b) represents data for $\langle g\rangle$ obtained from Eq. (2) using the same value of α. Considering only the BR effect, obviously an increase of $\langle g\rangle$ is expected in contrast to experiment. Here we have to correct for an isotropic g shift $g_0 = g_{00}(1+\beta k_F^2)$, as it may result from nonparabolicity [dash-dotted line in Fig. 4(b)]. Note, that the correction term with k^2 is also allowed by symmetry. In addition, β may contain also a contribution of the energy dependent penetration of the wave function into the SiGe bar-

rier. We can explain the observed dependence of $\langle g \rangle$ on n_s by including on top of the Rashba term this nonparabolicity correction using a value of $\beta = -5.4 \times 10^{-17}$ cm^2. The value of $\langle g \rangle$ extrapolated for zero concentration is $g_{00} = 2.00073 \pm 0.00010$. This value corresponds actually to the bottom of the lowest electron subband in the well and it refers only to electrons having the light mass. It is considerably bigger than that given by Feher[21] for heavily doped Si:P bulk material ($g_{\mathrm{Si}} = 1.99875 \pm 0.00010$). This difference is a consequence of nonparabolicity, barrier effects and the longitudinal mass contribution.

C. Line broadening and transverse relaxation

The field $\mathbf{H}_{\mathrm{BR}}$ is perpendicular to the $\mathbf{k}$ vector of the electron under consideration. Since the Fermi wave vector $\mathbf{k}_F$ may have any direction in the 2D plane, the BR field also has any direction in plane. Since the direction of $\mathbf{H}_{\mathrm{BR}}$ is randomly distributed within the 2D layer the resonance of the electrons occurs at different external fields. As a result, the line becomes broadened by the BR spin-orbit coupling. Neglecting both momentum scattering and cyclotron motion (weak field regime), one could expect that the linewidth broadening due to the BR effect would be described by the variance of the magnetic field seen by the electrons as described by Eq. (1). A change of the electron momentum, which is equivalent to a change of the BR field, leads, however, to an averaging of the linewidth. If the characteristic frequency of modulation is much higher than the frequency corresponding to the resonance linewidth, then the standard formula for motional narrowing, as used in this context first by D'yakonov and Perel (DP), can be applied.[14,15] Taking the angular dependence also into account we obtain

$$\Delta H = \gamma \delta H_{\mathrm{BR}}^2 \tau_k = \frac{\gamma H_{\mathrm{BR}}^2 \sin^2 \Theta}{2} \tau_k . \tag{3}$$

Here $\gamma = g \mu_B / \hbar$ is the gyromagnetic ratio and τ_k the momentum relaxation time. The observed angular dependence $\propto \sin^2 \Theta$ [see inset in Fig. 5(a)] is well described by Eq. (3) and it is a unique attribute of the discussed broadening mechanism where the fluctuating field has only an in-plane component.

From the experimental data for the CR linewidth [Fig. 5(b)] we evaluate τ_k. Taking these data together with the linewidth ΔH, we can evaluate the BR field from Eq. (3). Results are also given in Fig. 6 (full symbols). Without any further fitting parameter we obtain good agreement with the data derived from the *g*-factor anisotropy.

The linewidth for in-plane orientation is almost temperature independent (see Fig. 3). This is a consequence of the weak temperature dependencies of the Fermi energy and of the electron mobility.

D. Inhomogeneous line broadening

For perpendicular field ($\Theta = 0$) the second moment of the distribution of the effective field vanishes [see Eq. (3)] and the DP-BR mechanism of line broadening does not contribute anymore. For perpendicular orientation of the external magnetic field only another broadening is seen which is caused by the longitudinal spin relaxation or by the sample inhomogeneity. The longitudinal relaxation rate, as estimated from the saturation of the resonance signal at high microwave power[22] is only one of the contributions to the line broadening. Another one originates from the fluctuation of the Fermi *k* vector, that causes a variation in the *g* factor and thus an inhomogeneous distribution of the resonance field. Some samples, especially multi-quantum-well samples, where the electron concentration in the individual wells is different and those with low mobility exhibit much larger linewidths than those of Fig. 2.

The observed narrowing of the linewidth with increasing temperature (see Fig. 3, perpendicular field) shows that a considerable fraction of the inhomogeneous broadening is caused by a dependence of the resonance field on kinetic energy. With increasing temperature inelastic scattering of conduction electrons occurs and the kinetic energy varies in time leading to motional narrowing of the linewidth. Some contribution to the inhomogeneous linewidth may also originate from interface imperfections, which strongly affect the BR coefficient.

IV. CONCLUSION

We have shown that CESR measurements provide a very sensitive tool to evaluate the BR constant. The BR field is the origin of the observed anisotropies of the *g* factor and of the CESR linewidth. Both of them increase with increasing carrier density. Extrapolating the mean *g* value for low carrier density we find the subband edge *g* factor of 2D electrons in Si, $g_{00} = 2.00073 \pm 0.00010$. For perpendicular field the DP-BR linewidth broadening vanishes and the CESR is easiest to observe for that orientation.

In Si quantum wells we observe a very weak BR field because of weak spin orbit coupling. Therefore, spin relaxation is also very slow. The extremely small CESR linewidth (long dephasing time) and very long T_1 of the order of 10^{-5} s makes Si quantum wells an interesting candidate for spintronic devices.

ACKNOWLEDGMENTS

We thank F. Schäffler (JKU) for generously providing samples and helpful discussions. Work supported within the CELDIS in Poland and in Austria by the *Fonds zur Förderung der Wissenschaftlichen Forschung*, and ÖAD, both Vienna, and in Germany by the *Deutsche Forschungsgemeinschaft*.

[1] M. Dobers, K. v. Klitzing, and G. Weimann, Phys. Rev. B **38**, 5453 (1988).

[2] C. F. O. Graeff, M. S. Brandt, M. Stutzmann, M. Holzmann, G. Abstreiter, and F. Schäffler, Phys. Rev. B **59**, 13 242 (1999).

[3] Z. Wilamowski, N. Sandersfeld, W. Jantsch, D. Többen, and F. Schäffler, Phys. Rev. Lett. **87**, 026401 (2001).

[4] E. I. Rashba, Fiz. Tverd. Tela (Leningrad) **2**, 1224 (1969) [Sov. Phys. Solid State **2**, 1109 (1960)].

[5] Yu. L. Bychkov and E. I. Rashba, J. Phys. C **17**, 6039 (1984).
[6] S. Datta and B. Das, Appl. Phys. Lett. **56**, 665 (1990).
[7] See, e.g., S. Bandyopadhyay, Phys. Rev. B **61**, 13 813 (2000).
[8] M. I. D'yakonov and V. I. Perel', Sov. Phys. JETP **38**, 177 (1973); N. S. Averkiev and L. E. Golub, Phys. Rev. B **60**, 15 582 (1999).
[9] B. L. Altshuler and D. L. Maslov, Phys. Rev. Lett. **82**, 145 (1999); **83**, 2092 (1999).
[10] V. M. Pudalov, G. Brunthaler, A. Prinz, and G. Bauer, JETP Lett. **65**, 932 (1997); **68**, 442 (1998).
[11] D. Grundler, Phys. Rev. Lett. **84**, 6074 (2000).
[12] J. Luo and P. J. Stiles, Phys. Rev. B **41**, 7685 (1990).
[13] B. Jusserand, D. Richards, G. Allan, C. Priester, and B. Etienne, Phys. Rev. B **51**, 4707 (1995).
[14] F. G. Pikus and G. E. Pikus, Phys. Rev. B **51**, 16 928 (1995).
[15] W. Knap, C. Skierbiszewski, A. Zduniak, E. Litwin-Staszewska, D. Bertho, F. Kobbi, J. L. Robert, G. E. Pikus, F. G. Pikus, S. V. Iordanskii, V. Mosser, K. Zekentes, and Yu. B. Lyanda-Geller, Phys. Rev. B **53**, 3912 (1996).
[16] W. Jantsch, Z. Wilamowski, N. Sandersfeld, and F. Schäffler, Phys. Status Solidi B **210**, 643 (1998); Z. Wilamowski and W. Jantsch, Physica E (Amsterdam) **10**, 17 (2001).
[17] G. Feher, Phys. Rev. **114**, 1219 (1959).
[18] D. J. Bottomley, H. M. Van Driel, and J.-M. Baribeau, *Proceedings of the 22th International Conference on the Physics of Semiconductors*, Vancouver, 1994, edited by D. J. Lockwood (World scientific, Singapore, 1995), p. 1572.
[19] G. Lommer, F. Malcher, and U. Rössler, Phys. Rev. Lett. **60**, 728 (1988).
[20] E. I. Rashba and V. I. Sheka, in *Landau Level Spectroscopy*, edited by G. Landwehr and E. I. Rashba (Elsevier Science, Amsterdam, 1991).
[21] G. Feher, Phys. Rev. **114**, 1219 (1959).
[22] Z. Wilamowski and W. Jantsch, cond-mat/0112466 (unpublished).